NEURO

Aberrant functional connectivity of default-mode network in type 2 diabetes patients

Ying Cui[1] · Yun Jiao[1] · Hua-Jun Chen[1] · Jie Ding[1] · Bing Luo[1] · Cheng-Yu Peng[1] ·
Sheng-Hong Ju[1] · Gao-Jun Teng[1]

Abstract

Objectives Type 2 diabetes mellitus is associated with increased risk for dementia. Patients with impaired cognition often show default-mode network disruption. We aimed to investigate the integrity of a default-mode network in diabetic patients by using independent component analysis, and to explore the relationship between network abnormalities, neurocognitive performance and diabetic variables.

Methods Forty-two patients with type 2 diabetes and 42 well-matched healthy controls were included and underwent resting-state functional MRI in a 3 Tesla unit. Independent component analysis was adopted to extract the default-mode network, including its anterior and posterior components. Z-maps of both sub-networks were compared between the two groups and correlated with each clinical variable.

Results Patients showed increased connectivity around the medial prefrontal cortex in the anterior sub-network, but decreased connectivity around the posterior cingulate cortex in the posterior sub-network. The decreased connectivity in the posterior part was significantly correlated with the score on Complex Figure Test-delay recall test ($r=0.359$, $p=0.020$), the time spent on Trail-Making Test-part B ($r=-0.346$, $p=0.025$) and the insulin resistance level ($r=-0.404$, $p=0.024$).

✉ Gao-Jun Teng
  gjteng@vip.sina.com

[1] Jiangsu Key Laboratory of Molecular and Functional Imaging,
  Department of Radiology, Zhongda Hospital, Medical School of
  Southeast University, 87 Dingjiaqiao Road,
  Nanjing 210009, Jiangsu, China

Conclusion Dissociation pattern in the default-mode network was found in diabetic patients, which might provide powerful new insights into the neural mechanisms that underlie the diabetes-related cognitive decline.

Key points
• *Type 2 diabetes mellitus is associated with impaired cognition*
• *Default- mode network plays a central role in maintaining normal cognition*
• *Network connectivity within the default mode was disrupted in type 2 diabetes patients*
• *Decreased network connectivity was correlated with cognitive performance and insulin resistance level*
• *Disrupted default-mode network might explain the impaired cognition in diabetic population*

Abbreviations

T2DM	Type 2 diabetes
FMRI	Functional magnetic resonance imaging
BOLD	Blood oxygenation level-dependent
ICN	Intrinsic connectivity network
DMN	Default-mode network
aDMN	Anterior DMN
pDMN	Posterior DMN
FC	Functional connectivity
MPFC	Medial pre-frontal cortex
ACC	Anterior cingulate cortex
PCC	Posterior cingulate cortex
AD	Alzheimer's disease
ICA	Independent component analysis

MMSE	Mini-Mental State Examination
HAM-D	Hamilton Depression Rating Scale
OGTT	Oral glucose tolerance test
IR	Insulin Resistance
AVLT	Auditory Verbal Learning Test
CFT	Complex Figure Test
VFT	Verbal Fluency Test
TMT	Trail Making Test
CDT	Clock Drawing Test
FLAIR	Fluid-attenuated inversion recovery
WMH	White matter hyperintensity
MNI	Montreal Neurological Institute
IC	Independent component
ROI	Region of interest
FDR	False discovery rate
IPL	Inferior parietal lobule
SFG	Superior frontal gyrus

Introduction

Type 2 diabetes mellitus (T2DM) is associated with accelerated cognitive decline [1] and is a risk factor for dementia [2]. Recently, an increasing number of studies have provided significant insights into the structural and functional changes in the diabetic brain [3–5], which suggests the potential for neuroimaging to assist in understanding the pathways that might link T2DM to cognitive decrements.

Resting-state functional magnetic resonance imaging (rs-fMRI) has enabled the evaluation of brain functional architecture on the basis of blood oxygenation level-dependent (BOLD) signal, which represents the spontaneous neuronal activity at baseline state [6]. Resting-state networks, namely intrinsic connectivity networks (ICNs), are defined as brain regions with highly correlated time courses of low-frequency (<0.1 Hz) BOLD signal fluctuations [7]. Among these networks, the default-mode network (DMN) is the most widely studied and well-characterized one. Consisting of the medial pre-frontal cortex (MPFC), anterior cingulate cortex (ACC), posterior cingulate cortex (PCC) and precuneus [8], DMN is suggested as a major contributor to the normal cognitive functioning [9]. Reduction of intrinsic connectivity of the DMN has been observed in a number of mental disorders such as Alzheimer's disease (AD), autism, schizophrenia and hepatic encephalopathy [8, 10–12], which suggests its potential as a biomarker for clinical application. Given the impaired cognitive functioning in diabetic patients, we hypothesized that there might also be alterations in DMN connectivity in this population.

Independent component analysis (ICA), one of the multiple-regression methods, is a robust technique based on blind source separation that captures the essential components of multivariate rs-fMRI signals [13]. It helps to separate the whole-brain signal fluctuations from physiological noise and automatically capture the entire DMN as a single major component [14]. In comparisons with other analytical methods such as the seed-based method, ICA is proved to decrease the heterogeneity of DMN pattern by avoiding the a-priori seed selection, thus raising the reliability and reproducibility of the results [2].

In the present study, we adopted the ICA method to automatically identify DMN and explore its connectivity in T2DM patients. We aimed to evaluate (1) whether T2DM is associated with disrupted DMN compared with the healthy controls; and (2) whether the functional connectivity (FC) changes in the DMN are correlated with worse neurocognitive performance and T2DM-related parameters.

Methods

Participants

This study was approved by the local ethics committee and conducted between November 2012 and November 2013. Written informed consent was obtained from all participants. All subjects were between 50 and 75 years of age, right-handed and without any MR contraindication. A total of 43 patients were recruited by advertisements and met the latest criteria of T2DM [15]. All patients had a diabetes duration of at least 1 year. They were in close self-monitoring and routinely treated with various hypoglycaemic agents; none had any history of hypoglycaemic episodes. Healthy controls (n= 42) were also recruited through advertisements and were matched with T2DM patients with respect to age, sex and education. Exclusion criteria for both groups included an indication of dementia based on a Mini-Mental State Examination (MMSE) score ≤24 [16], history of depression based on the Hamilton Depression Rating Scale (HAM-D) score >7 [17], other psychiatric or neurological disorder unrelated to diabetes, a past history of alcohol or substance abuse, and brain lesions such as tumour or stroke. According to previous studies [18], we intentionally did not exclude subjects with vascular risk factors to raise the generalizability of our results.

Biometric measurement was performed at 8:00 a.m. All participants were recorded with detailed history of hypertension, smoking, medication and vascular disease. Laboratory parameters, such as fasting plasma glucose (FPG), fasting HbA1c, insulin and cholesterol were obtained and measured with standard laboratory testing. Subsequently, an oral glucose tolerance (OGTT) test (75 g dextrose monohydrate in 250 mL water) was performed on all healthy controls and patients without receiving treatment (n=8) to verify the diagnosis and severity of T2DM. Control subjects with fasting blood glucose level ≥7.0 mmol/L or 2-h postprandial glucose level≥7.8 mmol/L after OGTT test were excluded. During the

interview, blood pressure was measured at three different time points and averaged. Hypertension was defined as previously described [19]. HOMA-IR was used to determine the level of insulin resistance (IR) for all subjects, except for those with insulin treatment. Diabetic complications including the retinopathy and peripheral neuropathy were also measured to get a full picture of glycemic control in T2DM patients, using the same methods and criteria described elsewhere [20, 21].

Neuropsychological assessment

All participants performed an extensive neurocognitive examination covering several cognitive domains. All tests took approximately 60 min to complete. No medication was allowed immediately before the cognitive assessment. The MMSE and the HAM-D were used for excluding possible dementia and depression, respectively [16, 17]. The Auditory Verbal Learning Test (AVLT) and Rey-Osterrieth Complex Figure Test (CFT) (both included immediate recall and delayed recall tasks) were used for assessing episodic memory regarding either verbal or visual information [22, 23]. The Verbal Fluency Test (VFT) examines the semantic memory [24]. The Trail Making Test, parts A and B (TMT-A and TMT-B), was primarily used to evaluate attention and psychomotor speed [25]. The Clock Drawing Test (CDT) draws on a number of cognitive domains such as executive function and working memory [26].

Image acquisition and assessment

MRI data were acquired using a Siemens Verio 3.0-T system (Siemens, Erlangen, Germany) with a 12-channel head coil. All subjects had to refrain from taking medication before the MR. During imaging, subjects were covered with eye masks, instructed to remain awake and keep their heads still. Soft pads were used to reduce head movement and headphones were used to reduce noise. Functional images were obtained interleaved by using a gradient-recalled echo-planar (GRE-EPI) sequence (repetition time 2000 ms, echo time 25 ms, flip angle of 90°, field of view 240 mm×240 mm, acquisition matrix=64×64). A total of 240 whole-brain volumes were collected on 36 oblique slices with 4-mm thickness. Structural images were obtained by using a high-resolution T1-weighted 3D magnetization-prepared rapid gradient-echo imaging (3D MPRAGE) (176 slices, repetition time 1900 ms, echo time 2.48 ms, slice thickness 1.0 mm, flip angle of 9°, inversion time 900 ms, field of view 250×250 mm, in-plane resolution 256×256) for image registration and functional localization. Fluid-attenuated inversion recovery (FLAIR) images were obtained with the following parameters: repetition time 8500 ms, echo time 94 ms, 20 slices with 5-mm thickness, voxel size $1.3 \times 0.9 \times 5$ mm^3.

The white matter hyperintensity (WMH) on the FLAIR images was assessed using the age-related white matter changes scale [27]. Participants with a rating score of above one (confluence of lesions or diffuse involvement of the entire region) were excluded. Lacunar infarct was also assessed as well-defined areas of >2 mm with signal of cerebrospinal fluid.

Functional image processing and identification of DMNs

FMRI data preprocessing was carried out using SPM8 (Statistical Parametric Mapping, http://www.fil.ion.ucl.ac.uk/spm/). The following procedures were applied: slice timing adjustment; realignment for head motion correction (subjects with head motion >2.0-mm translation or >2.0° rotation were excluded); spatial normalization to standard Montreal Neurological Institute (MNI) template with a resampling voxel size of $3 \times 3 \times 3$ mm^3; spatial smoothing with a Gaussian kernel of 4 mm.

ICA was conducted using the Informix algorithm in the Group ICA of fMRI Toolbox (GIFT) software (Medical Image Analysis Lab, University of New Mexico, Albuquerque, NM, USA; http://icatb.sourceforge.net/). The number of independent components (ICs) was determined by using the minimum description length criteria and the mean dimension estimation was 25. Then, the averaged IC number was used for each subject for ICA decomposition. For each IC, the time courses correspond to the waveform of a specific pattern of coherent brain activity, and the intensity of this pattern of brain activity across the voxels is expressed in the associated spatial map. To display voxels relevant to each particular IC, the intensity values in each map were converted to z values. As previously described [12], the final DMN component was identified by visual inspection on the basis of periodic temporal fluctuation, spatial pattern, and distinct peak of power spectrum at low-frequency (<0.1 Hz) range.

Statistical analysis

The differences of clinical variables and cognitive performance between patients and the control group were examined by independent two-sample t test for continuous variables and $\chi 2$ test for proportions. Each comparison was performed with the SPSS software (version 18.0; SPSS, Inc., Chicago, IL, USA). $P<0.05$ was considered to be statistically significant.

To assess the within-group integrity of the best-fit components, one-sample t-tests were performed on the spatial maps of DMN for each group by using REST-Statistical Analysis (written by Chaogan Yan, www.restfmri.net) [28]. P values less than 0.05 were considered statistically significant. Multiple comparisons were performed by the relatively conservative false discovery rate (FDR) criterion to acquire the most significant results that mainly contain the DMN regions.

To explore the between-group differences, two-sample *t*-tests were performed on the spatial maps of the DMN in a voxel-by-voxel manner. To restrict the comparison to the voxels within the DMN only, we applied a mask that was created by combining the results obtained from one-sample *t*-test in each group. To exclude the possible confounding effects, age, sex and education level were included as covariates. Statistical threshold was set with $P<0.05$, combined with a minimum cluster size of 49 voxels for the anterior DMN, and 43 voxels for the posterior DMN for multiple comparison correction, resulted in a corrected $P<0.05$. To reflect the intrinsic abnormality of T2DM as much as possible, a less conservative correction was chosen that is determined by Monte Carlo simulation (AlphaSim program in AFNI, http://afni.nih.gov/afni/docpdf/AlphaSim.pdf) with the following parameters: single voxel, $P=0.05$; full width at half maximum, 4 mm; with the one-sample *t*-test results as the mask.

To investigate the relationship between DMN connectivity and clinical variables, Pearson correlation analyses were performed in a region of interest (ROI)-wise manner. Specifically, the ROI was defined as a spherical region within 6 mm of the peak activation in each brain region that differed significantly between the two groups. Then the mean z values of each ROI were correlated against the cognitive performance and T2DM-related variables in each patient. All analyses were performed using the SPSS software. P values<0.05 were considered statistically significant. To reduce the chance of type I error, a Bonferroni correction was performed for multiple comparisons.

To explore the effects of treatment modality in patients group, DMN pattern was first compared between patients with and without insulin therapy [29]. Next, we also explored the effects of diabetic complications by comparing the DMN pattern among the patients with neuropathy, retinopathy and those without complications. Finally, to determine whether these intergroup varieties could explain the DMN differences between T2DM patients and healthy controls, FC values were extracted from brain regions that differed significantly between groups and compared among all these sub-groups of patients.

Results

Participant information

One T2DM patient was excluded because of excessive head movement. Therefore, a total of 84 participants (42 T2DM patients and 42 healthy controls) were included in the final data analysis. Demographic and cognitive characteristics of all participants are presented in Table 1. Among the patients, 11 were treated with insulin, while the remainder were treated with either oral hypoglycaemic agents (n=23)or dietary restriction only (n=8). Clinical variables did not differ significantly between patients with and without insulin treatment, but the former tended to perform worse on several cognitive tests (supplementary Table 1). Comparing the diabetic and control groups, no significant differences were observed in terms of the total cholesterol, WMH loads and lacunar infarcts, and body mass index (BMI). However, patients performed significantly worse on the TMT-B and CFT-delayed recall tests, which mainly involved cognitive domains of executive function, processing speed and spatial episodic memory. Correlation analyses indicated that disease duration and HOMA-IR, instead of hyperglycaemic indices themselves (FPG and HbA1c), were the main contributors to these impaired performance (Supplementary Table 2).

Spatial patterns of DMN

Among the 25 components estimated during the data processing, two components were identified as the two sub-networks of DMN. A one-sample *t*-test showed the typical spatial pattern of each sub-network in both groups ($P<0.05$, FDR corrected) (Fig. 1). In the control group, the anterior DMN (Fig. 1, lower row) displayed functional connectivity (FC) mainly in the MPFC areas, as well as in the PCC/precuneus and small inferior parietal lobules (IPL) clusters. The posterior DMN (Fig. 1, lower row) showed FC within the PCC, precuneus and bilateral IPL regions, but also included a small part of MPFC. The DMN pattern of the patients largely included the same brain regions as the healthy controls.

Group differences in DMN

Compared with the healthy controls, patients showed increased FC in the anterior DMN region and decreased FC in the posterior DMN region ($P<0.05$, AlphaSim corrected). Specifically, the increased connectivity mainly involved bilateral superior frontal gyrus (SFG) (Fig. 2A). The decreased connectivity included the PCC and the precuneus (Fig. 2B). A detailed list of brain regions with aberrant FC in each sub-network is presented in Table 2.

DMN connectivity map was further compared between patients under insulin and non-insulin treatment, and between those with different diabetic complications. No significant difference was observed among these sub-groups of patients. Similarly, FC values extracted from the frontal region and the posterior regions also showed no significant difference among these sub-groups (Fig. 3A and B). However, insulin-treated patients suffered more functional alterations than those under non-insulin therapy, as shown in Fig. 3A.

Table 1 Demographic, clinical and cognitive characteristics

| Characteristics	T2DM Patients (n=42)	Control subjects (n=42)	P value
Age (years)	60.4±7.0	58.2±6.3	0.14
Sex (male)	23 (55)	14 (33)	0.08
Education (years)	9.6±3.8	10.2±2.3	0.35
Disease duration (years)	9.4±4.7	–	
Fasting glucose (mmol/L)[a]	7.8±2.1	5.5±0.4	<0.01
2-h postprandial glucose (mmol/L)[a]	15.5±4.2 (n=8)	6.5±1.7	<0.01
HbA1c (%)(mmol/mol)[a]	7.9±1.6 (62.7±17.4)	5.6±0.3 (37.8±3.6)	<0.01
HOMA-IR[a]	3.4±2.0	2.5±1.3	0.03
Blood pressure			
Systolic (mmHg)	136.6±14.7	132.7±15.0	0.23
Diastolic (mmHg)	85.8±11.3	86.8±11.4	0.70
Triglycerides (mmol/L)	1.46±0.80	1.41±0.87	0.77
Total cholesterol (mmol/L)	5.3±1.1	5.2±0.9	0.69
BMI (kg/m^2)	24.7±2.9	24.0±2.8	0.29
White matter lesions	1 (0–6)	0 (0–7)	0.28
Lacunar infarcts	9 (21)	5 (12)	0.38
Cognitive performance			
MMSE	28.3±1.1	28.7±1.2	0.11
Trail Making Test-A(s)	67.8±22.3	62.2±15.1	0.16
Trail Making Test-B(s)[a]	178.1±56.0	149.3±51.7	0.01
Auditory Verbal Memory Test	5.9±1.4	6.5±2.0	0.08
Auditory Verbal Memory Test-Delay Recall	5.7±2.5	6.3±2.2	0.20
Clock Drawing Test	3.3±0.6	3.5±0.5	0.10
Complex Figure Test-Immediate Recall	34.3±1.5	34.9±1.4	0.07
Complex Figure Test-Delayed Recall[a]	13.3±5.9	17.7±6.0	<0.01
Verbal Fluency Test	16.8±3.8	17.5±3.1	0.55
Hamilton Depression Rating Scale	1.7±1.0	1.2±0.8	0.20

Data are represented as mean±SD, n (%) or median (range). T2DM, type 2 diabetes mellitus

[a] P value <0.05
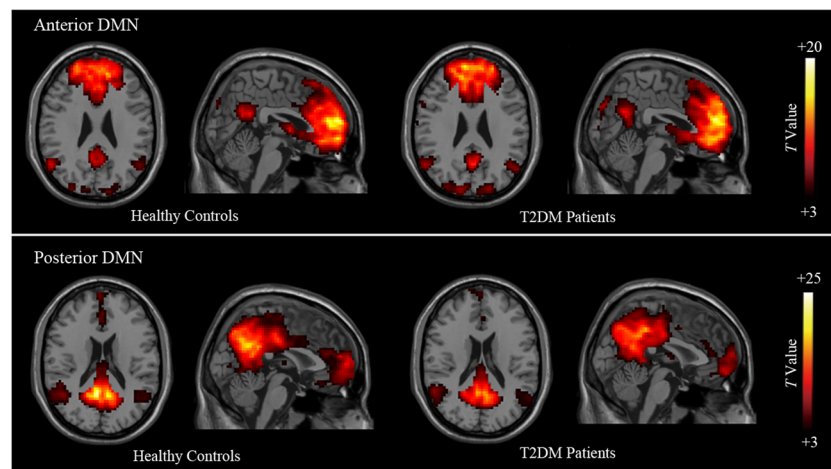
Fig. 1 Results of one-sample t-test of the two components representing the default-mode sub-networks in patients and healthy groups ($P<0.05$, FDR corrected). Representative images of the anterior default-mode network (DMN) (upper row) and the posterior DMN (lower row) in healthy controls and type 2 diabetes mellitus (T2DM) patients. Both components are displayed from the sectional and sagittal views. Colour scale represents t-values in each component ($P<0.05$, FDR corrected). DMN, default-mode network; T2DM, type 2 diabetes
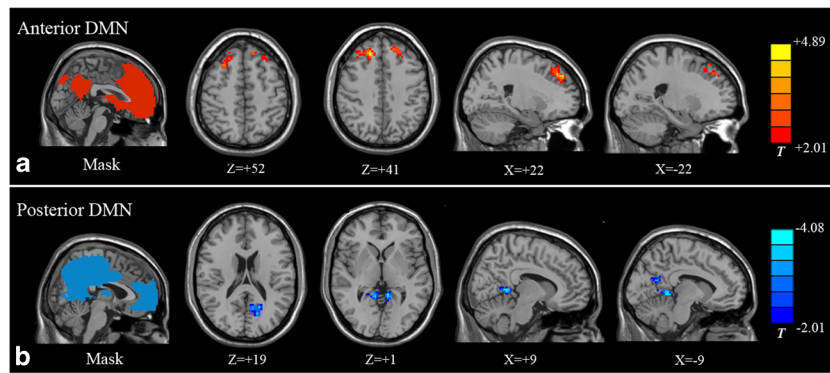
Fig. 2 Comparison of default-mode network (DMN) sub-networks between type 2 diabetes mellitus (T2DM) patients and healthy controls. (**A**) Compared with the healthy controls, patients with T2DM showed significantly increased FC (red colour) within the anterior DMN sub-network, predominantly in the right and the left SFG. (**B**) Decreased FC (blue colour) was found in the posterior sub-network of the DMN, which was mainly located around the retrosplenial regions such as the PCC and the precuneus. Pictures on the left column are masks of the two sub-components of DMN, obtained by combining results of one-sample t-test in each group, thresholding at $P<0.05$ (FDR corrected). Colour scale represents t-values. FC, functional connectivity; SFG, superior frontal gyrus; PCC, posterior cingulate cortex

Correlation analysis

FC strength in the pDMN was positively correlated with the CFT-delay and TMT-B performance, and negatively correlated with the insulin resistance level (Fig. 4). Specifically, the hypoconnectivity in the PCC region was related to higher insulin resistance level ($r=-0.404$, $p=0.024$) (Fig. 4B), while the mean z value in the precuneus had positive correlations with the CFT-delay score ($r=0.395$, $p=0.020$) and negative correlations with the time spent on TMT-B ($r=-0.346$, $p=0.025$) (Fig. 4C and D). No such correlations were observed in the control group (Supplementary Table 2). The treatment modality (with and without insulin) did not alter the significance of the associations between clinical variables and imaging parameters (Supplementary Table 3).

Table 2 Brain regions with significant differences on default-mode network (DMN) connectivity between type 2 diabetes mellitus (T2DM) patients and healthy controls

Brain region	BA	MNI coordinates			Cluster size	T value
		X	Y	Z		
Anterior DMN						
R superior frontal gyrus	9	18	33	42	188	+4.89
L superior frontal gyrus	8	−12	39	48	73	+3.15
Posterior DMN						
Precuneus	31	−15	−69	18	84	−3.40
Posterior cingulate cortex	30	9	−48	3	82	−4.08

BA, Brodmann area; MNI, Montreal Neurological Institute; X, Y, Z, coordinates of primary peak locations in the MNI space; L indicates the left; R indicates the right; positive t-values: T2DM > control subjects; negative t-values: T2DM < control subjects

Comparisons were performed at $P<0.05$, corrected for multiple comparisons

Discussion

Using the ICA method, we demonstrated a disrupted pattern of resting-state DMN in T2DM patients. Compared with healthy controls, T2DM patients showed increased FC within the aDMN regions while decreased FC within the pDMN regions. These functional alterations were related to the impaired cognitive performance and the increased insulin resistance level.

Evidence from recent fMRI studies suggested that the DMN anterior and posterior sub-networks interact in a dynamic equilibrium, which is important in the maintenance of normal cognition functioning [30]. However, with advancing age, this equilibrium is disrupted and these sub-networks develop greater independence from each other, thus resulting in their reciprocal changes [31]. Similar changes were also observed in other mental disorders, including Alzheimer's disease, ApoE 4 allele carriers, traumatic brain injury, major depression, epilepsy and autism [12, 31–36], suggesting that multiple disorders are linked to some analogous disruption of the DMN. Our study, for the first time, suggested this dissociation pattern in T2DM patients. Given its consistency across different mental disorders, this DMN dissociation pattern might be a potential imaging biomarker to identify T2DM patients with cognitive impairment. Furthermore, recent neuroimaging studies revealed that DMN changes could predict treatment response in mental disorders such as schizophrenia [37]. Therefore, this disrupted DMN signature also holds great potential to provide prognostic information for T2DM-associated cognitive decline.

Decreased connectivity was predominantly located in the PCC and the precuneus. These regions are the central nodes of the brain, the impairments of which are frequently treated as the early signs of cognitive impairment [38]. Neural dysfunction in these regions has been reported in the diabetic
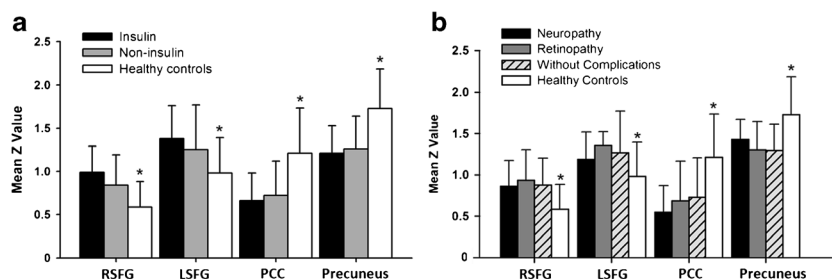
Fig. 3 Default-mode network (DMN) connectivity differences among different patients sub-groups and healthy controls. (A). The mean FC values extracted from the frontal regions in the diabetic group were significantly higher than the control group, while the mean FC values of the occipital lobe were significantly lower. There is a trend that patients with insulin treatment suffered more functional alterations than those without,

although the differences were not significant. (B) The mean FC value extracted from the frontal and the occipital lobe did not differ between the patients with and without diabetic complications. FC, functional connectivity; RSFG, right superior frontal gyrus; LSFG, left superior frontal gyrus; PCC, posterior cingulate cortex

population. For example, decreased neural intensity and coherence were detected around the precuneus regions [39]; decreased connectivity between the PCC and other nodes within the DMN was also observed [40]. Together with these previous findings, our results provided further evidence for the neural dysfunction in diabetes. Being correlated with cognitive performance, hypoconnectivity in these posterior regions might provide important insights into the neural mechanism underlying the impaired cognition in diabetic population. On the other hand, significantly increased connectivity was found in the bilateral superior frontal gyrus (SFG). Increased SFG activation has been reported previously in several depression-related fMRI studies, given that it is responsible for the modulation of emotional behavior and self-referential processing

[41]. T2DM is known to be associated with an increased risk of depression, which could lead to impaired self-consciousness and depressive symptoms [42]. We thus assume that the increased MPFC connectivity might be an early change that occurs before clinically measurable depression. Further studies including depressive T2DM patients are of particular interest to determine the clinical significances of our results.

Our results showed no correlations between the glycaemic control and functional changes, which was inconsistent with a previous PET/CT study [43]. It is important to note that whether hyperglycaemia is an independent risk factor for impaired cognition is still under debate [44]. As 'diabetic encephalopathy' is a multifactorial condition [45], the hyperglycaemia *per se* may not be the most important

Fig. 4 Correlations between clinical parameters and the mean z value extracted from significantly different brain regions. (A) Spherical regions of interest (ROIs) located in the precuneus and the PCC, and their coordinates of peak activation. (B) The mean z value of the ROI extracted from the PCC was negatively related to insulin resistance (R=0.404, P=0.024). (C) The mean z value of the ROI extracted from the precuneus was positively correlated with the CFT-delayed recall scores in the diabetic group (R=0.395, P=0.020). (D) The mean z value of the ROI extracted from the precuneus had negative correlations with the time spent on the TMT-B (R=-0.346, P=0.025). CFT, complex figure test; TMT-B, trail making test-part B; PCC, posterior cingulate cortex
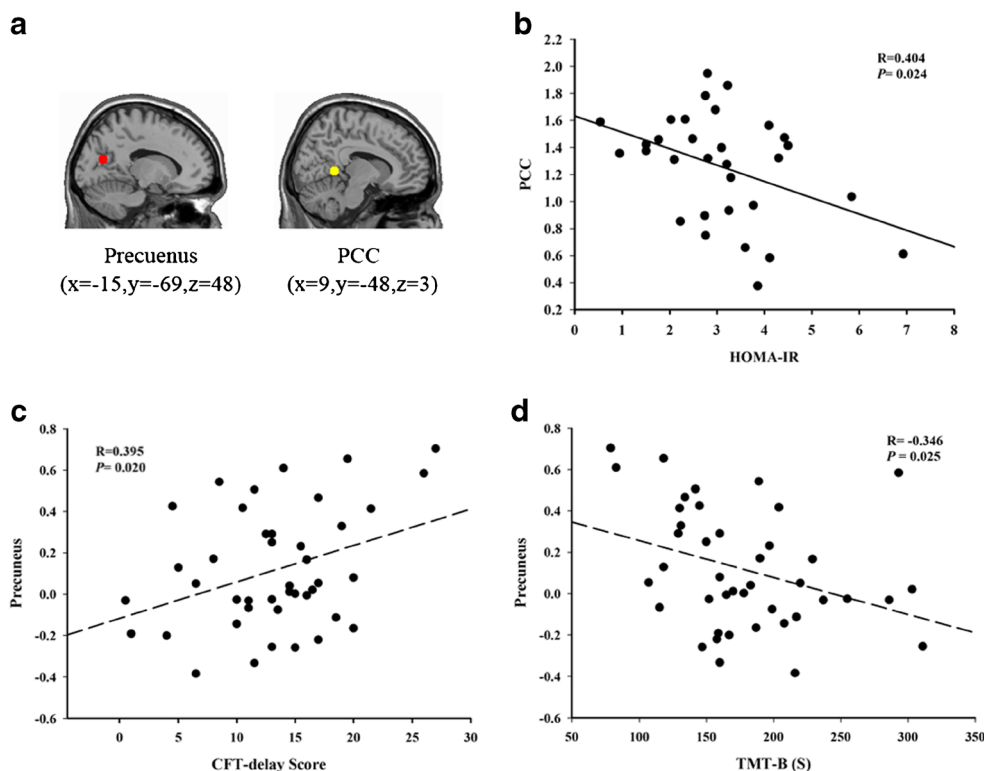
contributor for the cognitive impairment. In the current results, IR was independently correlated to DMN alterations (Fig. 4B). Recently, IR has been recognized as a promising determinant for cognitive decline, as it is tightly associated with Alzheimer's disease-like pathology [1]. Consistent with previous imaging studies [46, 47], our results suggested that IR might be more sensitive to detect neural alterations over other glycaemic indices. In addition, patients having insulin treatment suffered more functional abnormalities than those without (Fig. 3A). This is in accordance with previous large-scale clinical studies [48] supporting that insulin-treated patients have a higher risk for dementia, which is possibly mediated by more severe pathological changes and direct effects of insulin. A critical direction for future work is to explore the mechanism underlying T2DM associated cognitive decline. Further research with longitudinal design and less heterogeneity are warranted to achieve this goal.

We note that our study has several limitations. First, this study was limited to a relatively small sample size by using advertisement recruitment, which may to some extent reduce the generalizability of the results. Second, most of the included patients were variously medicated, making it difficult to determine whether some of our results were secondary to possible effects of medication. Medication-naïve subjects should be included in future studies to exclude such effects. Finally, we did not measure the serum glucose level just before the MR. Further studies should take it into consideration to better elucidate the relationship between glycaemic control and neural dysfunction.

In conclusion, the DMN connectivity was altered in T2DM patients, which was associated with impaired cognition and increased insulin resistance. In contrast to standard cognitive tests, using DMN as a potential screening tool for cognitive decline offers us an opportunity to observe the living brain in a non-invasive way. Future perspectives include application of fMRI techniques in longitudinal studies to define the evolution of DMN connectivity with the progression of T2DM, as well as the effects of various therapeutic approaches on central nervous system plasticity.

References

1. McCrimmon RJ, Ryan CM, Frier BM (2012) Diabetes and cognitive dysfunction. Lancet 379:2291–2299
2. Musen G, Jacobson AM, Bolo NR et al (2012) Resting-state brain functional connectivity is altered in type 2 diabetes. Diabetes 61:2375–2379
3. Reijmer YD, Brundel M, de Bresser J, Kappelle LJ, Leemans A, Biessels GJ (2013) Microstructural white matter abnormalities and cognitive functioning in type 2 diabetes: a diffusion tensor imaging study. Diabetes Care 36:137–144
4. Marder TJ, Flores VL, Bolo NR et al (2014) Task-induced brain activity patterns in type 2 diabetes: a potential biomarker for cognitive decline. Diabetes 63:3112–3119
5. Ryan JP, Fine DF, Rosano C (2014) Type 2 diabetes and cognitive impairment: contributions from neuroimaging. J Geriatr Psychiatry Neurol 27:47–55
6. Fox MD, Raichle ME (2007) Spontaneous fluctuations in brain activity observed with functional magnetic resonance imaging. Nat Rev Neurosci 8:700–711
7. Rosazza C, Minati L (2011) Resting-state brain networks: literature review and clinical applications. Neurol Sci 32:773–785
8. Buckner RL, Andrews-Hanna JR, Schacter DL (2008) The brain's default network: anatomy, function, and relevance to disease. Ann N Y Acad Sci 1124:1–38
9. Smucny J, Wylie KP, Tregellas JR (2014) Functional magnetic resonance imaging of intrinsic brain networks for translational drug discovery. Trends Pharmacol Sci 35:397–403
10. Adriaanse SM, Sanz-Arigita EJ, Binnewijzend MA et al (2014) Amyloid and its association with default network integrity in Alzheimer's disease. Hum Brain Mapp 35:779–791
11. Zhang L, Qi R, Wu S et al (2012) Brain default-mode network abnormalities in hepatic encephalopathy: a resting-state functional MRI study. Hum Brain Mapp 33:1384–1392
12. Zhou Y, Milham MP, Lui YW et al (2012) Default-mode network disruption in mild traumatic brain injury. Radiology 265:882–892
13. De Luca M, Beckmann CF, De Stefano N, Matthews PM, Smith SM (2006) fMRI resting state networks define distinct modes of long-distance interactions in the human brain. NeuroImage 29:1359–1367
14. Greicius MD, Krasnow B, Reiss AL, Menon V (2003) Functional connectivity in the resting brain: a network analysis of the default mode hypothesis. Proc Natl Acad Sci U S A 100:253–258
15. American Diabetes Association (2013) Diagnosis and classification of diabetes mellitus. Diabetes Care 36:S67–S74
16. Galea M, Woodward M (2005) Mini-Mental State Examination (MMSE). Aust J Physiother 51:198
17. Hamilton M (1960) A rating scale for depression. J Neurol Neurosurg Psychiatry 23:56–62
18. Manschot SM, Brands AM, van der Grond J et al (2006) Brain magnetic resonance imaging correlates of impaired cognition in patients with type 2 diabetes. Diabetes 55:1106–1113
19. van den Berg E, Kloppenborg RP, Kessels RPC, Kappelle LJ, Biessels GJ (2009) Type 2 diabetes mellitus, hypertension,

dyslipidemia and obesity: a systematic comparison of their impact on cognition. Biochim Biophys Acta 1792:470–481

20. Klein R, Klein BE, Magli YL et al (1986) An alternative method of grading diabetic retinopathy. Ophthalmology 93:1183–1187

21. Ryan CM, Geckle MO (2000) Circumscribed cognitive dysfunction in middle-aged adults with type 2 diabetes. Diabetes Care 23:1486–1493

22. Schmidt M (1996) Rey auditory verbal learning test: a handbook. Western Psychological Services, Los Angeles

23. Shin MS, Park SY, Park SR, Seol SH, Kwon JS (2006) Clinical and empirical applications of the Rey-Osterrieth Complex Figure Test. Nat Protoc 1:892–899

24. Brucki SM, Rocha MS (2004) Category fluency test: effects of age, gender and education on total scores, clustering and switching in Brazilian Portuguese-speaking subjects. Braz J Med Biol Res 37:1771–1777

25. Bowie CR, Harvey PD (2006) Administration and interpretation of the Trail Making Test. Nat Protoc 1:2277–2281

26. Samton JB, Ferrando SJ, Sanelli P, Karimi S, Raiteri V, Barnhill JW (2005) The clock drawing test: diagnostic, functional, and neuro-imaging correlates in older medically ill adults. J Neuropsychiatry Clin Neurosci 17:533–540

27. Wahlund LO, Barkhof F, Fazekas F et al (2001) A new rating scale for age-related white matter changes applicable to MRI and CT. Stroke 32:1318–1322

28. Song XW, Dong ZY, Long XY et al (2011) REST: a toolkit for resting-state functional magnetic resonance imaging data processing. PLoS One 6, e25031

29. American Diabetes Association (2014) Executive summary: standards of medical care in diabetes—2014. Diabetes Care 37:S5–S13

30. Uddin LQ, Kelly AM, Biswal BB, Castellanos FX, Milham MP (2009) Functional connectivity of default mode network components: correlation, anticorrelation, and causality. Hum Brain Mapp 30:625–637

31. Jones DT, Machulda MM, Vemuri P et al (2011) Age-related changes in the default mode network are more advanced in Alzheimer disease. Neurology 77:1524–1531

32. Zhu X, Wang X, Xiao J et al (2012) Evidence of a dissociation pattern in resting-state default mode network connectivity in first-episode, treatment-naive major depression patients. Biol Psychiatry 71:611–617

33. Starck T, Nikkinen J, Rahko J et al (2013) Resting state fMRI reveals a default mode dissociation between retrosplenial and medial prefrontal subnetworks in ASD despite motion scrubbing. Front Hum Neurosci 7:802

34. Jones DT, Vemuri P, Murphy MC et al (2012) Non-stationarity in the "resting brain's" modular architecture. PLoS One 7, e39731

35. Andrews-Hanna JR, Snyder AZ, Vincent JL et al (2007) Disruption of large-scale brain systems in advanced aging. Neuron 56:924–935

36. Machulda MM, Jones DT, Vemuri P et al (2011) Effect of APOE epsilon4 status on intrinsic network connectivity in cognitively normal elderly subjects. Arch Neurol 68:1131–1136

37. Tregellas JR, Tanabe J, Rojas DC et al (2011) Effects of an alpha 7-nicotinic agonist on default network activity in schizophrenia. Biol Psychiatry 69:7–11

38. Leech R, Sharp DJ (2014) The role of the posterior cingulate cortex in cognition and disease. Brain 137:12–32

39. Cui Y, Jiao Y, Chen YC et al (2014) Altered spontaneous brain activity in Type 2 diabetes: a resting-state functional MRI study. Diabetes 63:749–760

40. Hoogenboom WS, Marder TJ, Flores VL et al (2014) Cerebral white matter integrity and resting-state functional connectivity in middle-aged patients with type 2 diabetes. Diabetes 63:728–738

41. Sheline YI, Barch DM, Price JL et al (2009) The default mode network and self-referential processes in depression. Proc Natl Acad Sci U S A 106:1942–1947

42. Musselman DL, Betan E, Larsen H, Phillips LS (2003) Relationship of depression to diabetes types 1 and 2: epidemiology, biology, and treatment. Biol Psychiatry 54:317–329

43. Busing KA, Schonberg SO, Brade J, Wasser K (2013) Impact of blood glucose, diabetes, insulin, and obesity on standardized uptake values in tumors and healthy organs on 18F-FDG PET/CT. Nucl Med Biol 40:206–213

44. Euser SM, Sattar N, Witteman JC et al (2010) A prospective analysis of elevated fasting glucose levels and cognitive function in older people: results from PROSPER and the Rotterdam Study. Diabetes 59:1601–1607

45. Van den Berg E, Kessels R, Kappelle L et al (2006) Type 2 diabetes, cognitive function and dementia: vascular and metabolic determinants. Drugs Today (Barc) 42:741–754

46. Baker LD, Cross DJ, Minoshima S et al (2011) Insulin resistance and Alzheimer-like reductions in regional cerebral glucose metabolism for cognitively normal adults with prediabetes or early type 2 diabetes. Arch Neurol 68:51–57

47. Willette AA, Xu G, Johnson SC et al (2013) Insulin resistance, brain atrophy, and cognitive performance in late middle-aged adults. Diabetes Care 36:443–449

48. Ott A, Stolk R, Van Harskamp F et al (1999) Diabetes mellitus and the risk of dementia The Rotterdam Study. Neurology 53:1937–1942